

COMPLIANCE REAL TIME MONITORING IN MODE II DELAMINATION FATIGUE TESTS

J. Vicens ¹, J. Costa ¹, J. Renart ¹

¹ AMADE. Analysis and Advanced Materials for Structural Design,
Escola Politècnica Superior, EPS. Universitat de Girona, UdG,
Campus Montilivi s/n. 17071 Girona, Spain
E-mail: pep.vicens@udg.edu

ABSTRACT

An experimental investigation of crack growth under fatigue loading on epoxy resin reinforced with unidirectional carbon fibre and which focuses on the introduction of a new methodology based on real-time monitoring of the compliance is presented. The new methodology is based on a new definition of the compliance as the ratio of load and displacement amplitudes applied in fatigue tests. This new definition allows the value of the compliance of the specimen, in spite of the non-linearities introduced by fixtures and load application during the test, to be obtained. In the experimental program to validate the new methodology, 3ENF fatigue tests were carried out to obtain the onset of crack growth and the associated da/dN - G_{max} curves for ratio $R=0.1$ and 5 Hz frequency. The fatigue tests were carried out for different G_C rates (10%, 20%, 30%, 40%, etc.). Onset curve and crack growth rate for AS4/3501 are presented.

KEY WORDS: fatigue, crack growth, three point bending, end notched flexure, real time monitoring, compliance.

1. INTRODUCTION

Nowadays, the information provided by fatigue tests, the onset point (initiation of crack growth) and crack growth rate (evolution of the crack once it has started), requires long duration tests, which are labour intensive. All the information is provided by the study of the evolution of the specimen's compliance and/or the measure of the crack length. For fatigue tests in mode I [1] a variation of 1% or 5% of the compliance is considered as an indication of crack onset. The normalized procedure to obtain the onset point requires stopping the test periodically to carry out static tests on the lineal zone of the material in order to evaluate the specimen's compliance. The accuracy of this method depends on the frequency of the stops, and requires the continuous intervention of the technician. Therefore, the fatigue tests become extremely costly and produce scattered results.

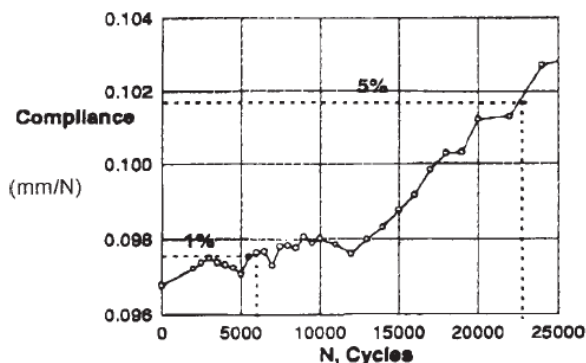


Figure 1. Evolution of the compliance in front of the Number of cycles. ASTM D6115 – 97 p:5.

To attain the crack growth rate, the crack length have to be measured by visual inspection along the specimen edges. A set of $a(N)$ points are then obtained. Ideally, the crack growth rate da/dN corresponds to the derivate of the $a(N)$ curve of the specimen. Great efforts have been made to automate fatigue procedures in composites with the aim of determining the damage evolution on real time. Some authors have proposed different methodologies to determine the damage onset point. For example, acoustic emissions [2], optical fibre sensors [3] or a variation of the conductivity of the material [4] have been some solutions presented. These methods require a lot of time for specimen preparation and involve the use of sensors for the test.

In this work a methodology to determine the fatigue crack growth behaviour (onset and crack growth rates) of delamination in composite materials is presented. This methodology is based on the real-time monitoring of the specimen compliance.

2. EXPERIMENTAL

Composite material manufactured from 3501 resin reinforced with unidirectional carbon fibres AS4 cured in an autoclave under standard aeronautical conditions was used. The laminate configuration consists of 16 plies with 0° orientation /insert/ 16 plies with 0° orientation, employing a PTFE foil insert of $30\mu\text{m}$ of thickness and 60 mm length in order to produce an artificial delamination to initiate the crack in the mid plane. The samples were approximately 25mm wide, 5.5mm thick and 210mm long approximately.

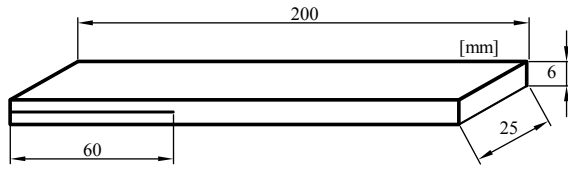


Figure 2. Specimen dimensions.

17 samples have been tested to obtain the onset curve. For this experimental program validation in mode II a variation of 2% of the compliance is considered to indicate crack onset. The limit for the initiation of the crack growth has been considered as 2.5 million cycles. The $da/dN-G_{max}$ graph has been built up with the information provided by the 10%Gc to 50%Gc samples. All tests have been carried out at $R=0.1$ and 5Hz frequency.

Table 1. Initial conditions for fatigue tests in $R=0.1$.

# samples	%Gc	δ_{min} [mm]
2	10	-0.370
3	20	-0.524
3	30	-0.642
2	40	-0.741
3	50	-0.828
2	70	-0.980
2	90	-1.111

A three point bending, 3ENF, fixing tool has been used to reproduce the mode II testing conditions used in this study. The parameters of the fixing tool were $L=50\text{mm}$ (distance between the load applicator and roller support) and an initial crack length of 25mm (distance from the end to the insert and the roller support).

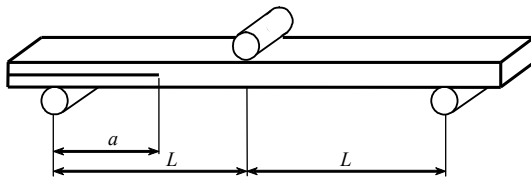


Figure 3. 3ENF fixing tool.

A clip-on-gage extensometer Epsilon 3541-008M-025M has been used to measure the displacement values. The fatigue tests were carried out under displacement control.

3. DYNAMIC COMPLIANCE

The compliance of any structural component is defined by LEFM as the ratio between displacement and load, $C=\delta/P$. Assuming a perfect linear behaviour of the material, the compliance value is the slope on a load-displacement graph assuming the it passes through the origin of coordinates. The value of the slope remains constant until any damage on the material occurs (matrix cracking, fibre breaks, fibre kinking, delamination...)

and thus provokes a variation of the slope. Any non-linear effect causes a loss of stiffness in the material. When the material is being damaged the value of the compliance varies, it can increase suddenly as in a sudden crack growth in delamination tests or it can be noticed as a smooth loss of linearity as in the formation of micro-cracks.

The geometry and manufacture of the three point bending fixing tool used in this study introduces a non-linearity at small displacements. The slope on the load-displacement increases in the initial zone until it reaches a constant slope value corresponding to the value of compliance of the specimen tested. Plays between pieces of the fixing tool, an inaccurate load introduction on the specimen or geometrical non-linearities of the samples are the principal causes that produce these non-linearities.

Due to the initial non-linearity produced by the fixing tool, the implementation of the LEFM definition to calculate the compliance during a fatigue test exhibits uncertainty on the compliance value. In fatigue tests, controlled by displacement, cyclic displacement following a sinus wave is applied producing a corresponding sinus wave force response. In figure 4 the displacement δ' and δ'' applied corresponds to point A and point B respectively on the displacement-force curve. The compliance calculated as LEFM definition, the slope between the chosen point and the origin of coordinates, gives different values depending on the chosen point. The compliance during dynamic tests does not remain constant and varies from the minimum value, C' , (corresponding to the minimum displacement), to a maximum value of compliance, C'' .

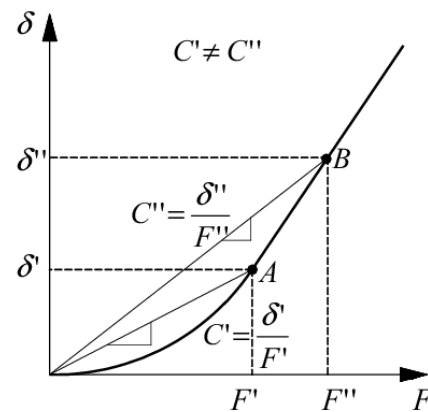


Figure 4. Classical definition of Compliance.

In an attempt to avoid the effect of the initial non-linearity a new definition to calculate the compliance is proposed. The idea begins by defining the compliance as the ratio between the displacement amplitude and load amplitude applied during a cyclic period in a dynamic test.

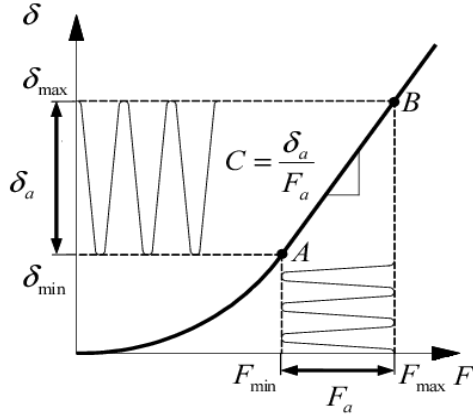


Figure 5. New definition of compliance.

The definition of the compliance corresponds to the secant line between two points in any shape of the load-displacement curve. On a fatigue test controlled by displacement, the displacement signals are set up at the beginning of the test. In Figure 5 the minimum displacement, δ_{\min} , and the maximum displacement, δ_{\max} , are chosen to produce on the sample a, F_{\min} , and F_{\max} , respectively at a chosen frequency. The newly calculated compliance is the slope of the line that connects point B and point A and corresponds to the ratio of the displacement amplitude, δ_a , and force, F_a .

The amplitude of both, force and displacement can be calculated from the instantaneous signals provided by the load cell and extensometer following the outlined procedure below:

The sensors of force and displacement acquire signals which follow a sinus wave form (see equation 1 and 2).

$$F(t) = F_m + F_a \sin\left(\frac{2\pi}{T}t + \theta\right) \quad (1)$$

$$\delta(t) = \delta_m + \delta_a \sin\left(\frac{2\pi}{T}t\right) \quad (2)$$

Where, F_m and δ_m are the mean value of load and displacement, F_a and δ_a are the actual amplitude of force and displacement respectively. T , is the period of one cycle and, t , is the time.

$$F^2(t) = F_m^2 + F_a F_m \sin\left(\frac{2\pi}{T}t\right) + F_a^2 \sin^2\left(\frac{2\pi}{T}t\right) \quad (3)$$

$$\delta^2(t) = \delta_m^2 + \delta_a \delta_m \sin\left(\frac{2\pi}{T}t\right) + \delta_a^2 \sin^2\left(\frac{2\pi}{T}t\right) \quad (4)$$

$$\int_0^T F^2(t) dt = \int_0^T F_m^2 dt + \int_0^T F_a F_m \sin\left(\frac{2\pi}{T}t\right) dt + \int_0^T F_a^2 \sin^2\left(\frac{2\pi}{T}t\right) dt \quad (5)$$

$$\int_0^T \delta^2(t) dt = \int_0^T \delta_m^2 dt + \int_0^T \delta_a \delta_m \sin\left(\frac{2\pi}{T}t\right) dt + \int_0^T \delta_a^2 \sin^2\left(\frac{2\pi}{T}t\right) dt \quad (6)$$

Secondly, to obtain equations function of the mean and the amplitude value the equations 1 and 2 have to be squared. By squaring these equations the signal-noise from the sensors is also squared. A robust method to calculate the new compliance is required particularly after squaring the signals acquired and the noise of the values. The integration of the sinus wave form signal during one period, T , provides an averaged value and reduces the signal-noise ratio and so providing a robust method to obtain the compliance.

$$F_a^2 = \frac{\int_0^T F^2(t) dt - F_m^2 T}{\pi} \quad (7)$$

$$\delta_a^2 = \frac{\int_0^T \delta^2(t) dt - \delta_m^2 T}{\pi} \quad (8)$$

Finally, the Dynamic Compliance (DC) is defined as the ratio between the square root of the amplitudes of displacement and load found in equations 7 and 8.

$$C = \frac{\delta_a}{F_a} \quad (9)$$

The Dynamic Compliance is implemented on the control software of the MTS servo-hydraulic testing machine. The algorithm calculates the values of the new compliance from the input signals (force and displacement) from the sensors (load cell and extensometer). The algorithm is based on arithmetic operations and recalculates the value of the compliance every clock interval between each response of the servovalve allowing a real time monitoring compliance that can be stored or visualized to be obtained.

3.1 Experimental Compliance Calibration

To determine the crack length, it is necessary to obtain the crack growth length, and so the Experimental Compliance Calibration, CCE, is used in spite of the visual crack determination. The crack length and the sample compliance are correlated in a lineal relation between the compliance and the crack length cubed.

Load and unload testing in the elastic range for different crack lengths provides the information required to determine the slope, m , of the regression line on a C in front of a^3 graph. ESIS [5] proposes a complete characterization of the compliance using 0, 15, 20, 25, 30, 35, 40mm of crack length. Implementing the values of the regression line obtained permits the crack length on real time to be obtained.

ESIS standard for static test in mode II proposes static test on elastic range before testing to determine the Experimental Compliance Calibration, CCE. This paper

proposes calculating the CCE using dynamic tests in spite of static tests for different crack length because the tests simulate the same fatigue testing conditions on the sample and allow the use of the dynamic compliance, DC, to obtain the different compliance values consequently reducing the testing time spent.

Static and dynamic test were carried out on the same sample to compare the static and dynamic values of, m for an Experimental Compliance Calibration for different ranges of energy release rates. The sample between one static test and the dynamic test remains on the fixing tool without moving ensuring the exact same test conditions are repeated. The static test was carried out on the elastic range and the dynamic test between the displacements that produce different energy release rates with a ratio of $R=0.1$.

Figure 6 shows the slopes of compliance in function of crack length cubed for first order polynomial regression of the static values on the elastic range, m_{st} . Figure 7 depicts the first order polynomial regression line of the load-displacement dynamic test values, m_{dyn} ; and in figure 8 the new method of dynamic compliance, DC, calculated directly from the testing machine, m_{DC} .

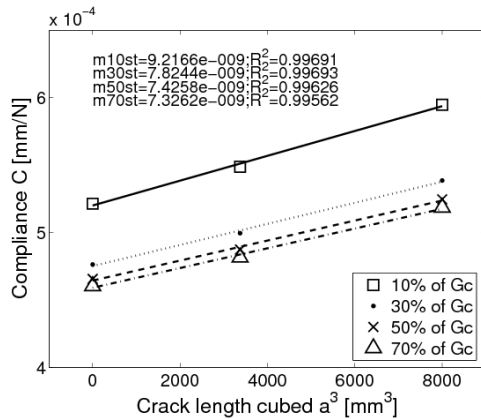


Figure 6.CCE Static Compliance Calibration $R=0.1$.

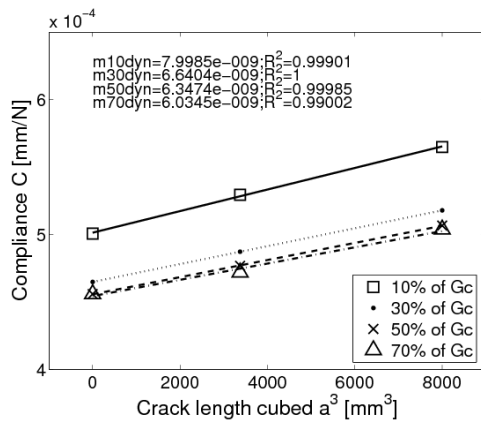


Figure 7.Registration Dynamic Compliance Calibration $R=0.1$.

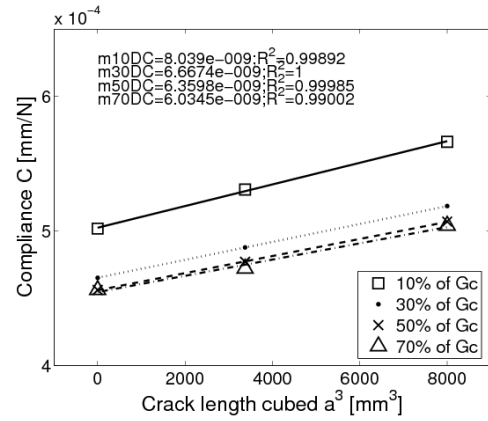


Figure 8.DC Calibration $R=0.1$.

The slope results using the same method are summarized in table 1. The difference between the static and dynamics results of the compliance calibration is about 15%. The values obtained with the new method proposed in this paper are practically equal to those obtained with the first order polynomial regression line of the load- displacement of the dynamic values for all the cycles of the dynamic test.

Table 2. Comparison of results of static and dynamic experimental compliance calibration.

%G	m_{st}	$m_{dyn}(\text{regression})$	m_{DC}
10	9.216e-9	7.998e-9	8.039e-9
30	7.824e-9	6.640e-9	6.667e-9
50	7.425e-9	6.347e-9	6.360e-9
70	7.326e-9	6.034e-9	6.034e-9
mean	7.948e-9	6.755e-9	6.775e-9

In conclusion, the standard method proposed by ESIS [5] to calculate the compliance calibration is not useful in fatigue test because it does not take into account the fatigue test conditions.

3.2 Range of use

When the Dynamic Experimental Compliance Calibration, CCEdyn, is carried out, the effect of the number of cycles on the specimen have to be taken into consideration because the cycles applied have to be added later, (i.e. after the running the test), to the value of the onset point. Besides, the number of cycles applied to the sample at low rates of energy release rate does not damage the specimen. However, for fatigue tests at rates of energy release rate close to the critical energy release rate a few cycles could damage the sample even when the CCEdyn is done.

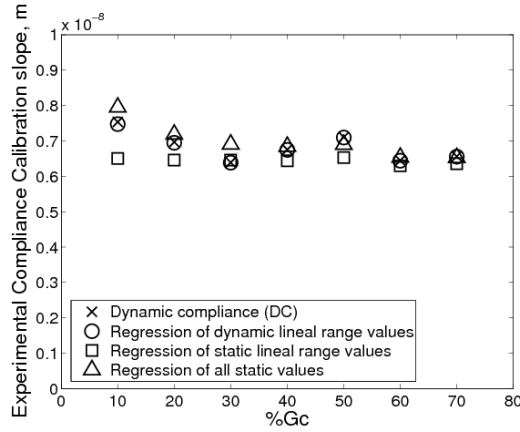


Figure 9. Comparison of parameter m in function of $\%G_c$.

Figure 9 compares the slope of the CCE for different $\%G_c$ and different calculation methods. The most constant method in front of the variation of the G_c is the one based on the LEFM method. This method calculates the slope as a regression of all the values of the constant slope of a displacement force graph. The DC method gives similar values in the range of 30 to 70 % of G_c . This range allows carrying out the CCE for each sample independent of which conditions will be tested. The option to choose the rate of G_c to calculate the CCE avoids the effects of fixing tool non-linearities at low rates of G_c or damaging the sample at close G_c rates.

4. RESULTS AND DISCUSSION

The experimental results obtained are presented.

4.1 Experimental result for sample

The new dynamic compliance (DC) allow the storage of the experimental values of every cycle providing a nearly continuous $C(N)$ and $a(N)$ graph if the CCE is used in the second case. The door is open to improve the accuracy in the determination of the onset point and the determination of the da/dN - G_{max} graph. Furthermore, man-labour dependence is drastically reduced achieving a virtually automatic fatigue test.

Figure 10 shows the experimental data results for one test. At least one hundred cycles are required to reach a constant value of DC because the extensometer requires some cycles to reach the command values. The compliance remains constant until the sample is damaged. The onset point is calculated as the intersection between the 2% compliance variation line and the DC values. The accuracy of the determination on the onset point depends on the frequency of the cycles stored.

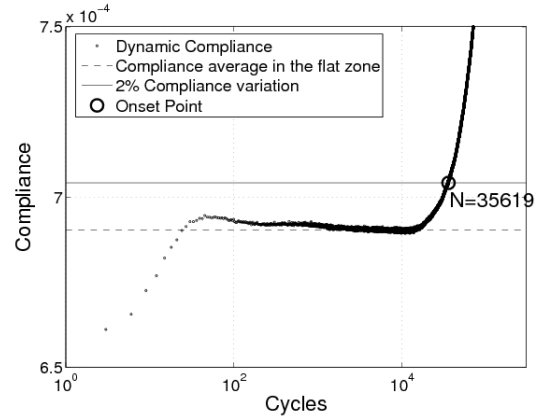


Figure 10. Compliance-cycle graph for 5L41G04 specimen.

4.2 Beginning of delamination

Figure 11 presents the fatigue curve characterization of the material (crack growth onset). The curve is obtained by adjusting the experimental data.

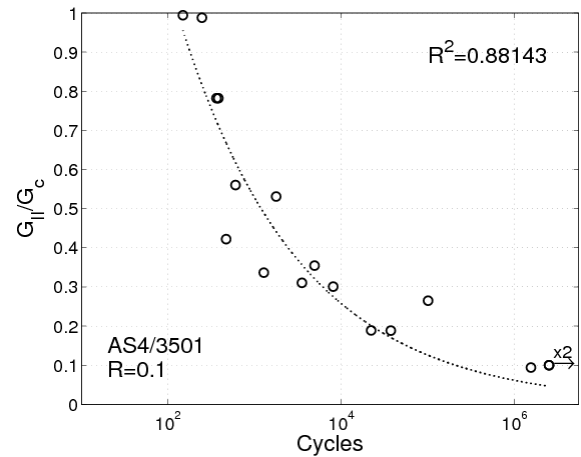


Figure 11. Onset curve for AS4/3501.

The energy release rate of each specimen in figure 11 is different to the initial conditions in table 1. The initial test conditions are calculated based on information provided by static tests. The experimental $\%G$ is calculated using experimental values (initial crack length, force) in every cycle by:

$$G_{\max} = \frac{3mF_{\max}^2 a^2}{2B} \quad (10)$$

The new methodology presented in this paper allows real test fatigue conditions to be calculated more accurately.

4.3 da/dN - G_{\max} curve

The calculation of da/dN is not a direct result. From the real time compliance stored and by using the

experimental compliance calculation the crack length in front of cycles graph is obtained. The velocity of the crack growth is the slope of the a vs N graph. The slope is calculated by using a first degree polynomial regression for different vector length of a and N . The maximum energy release rate is calculated from the crack length and force values of the vectors, used to calculate the slope, using equation 10. Figure 12 shows the result.

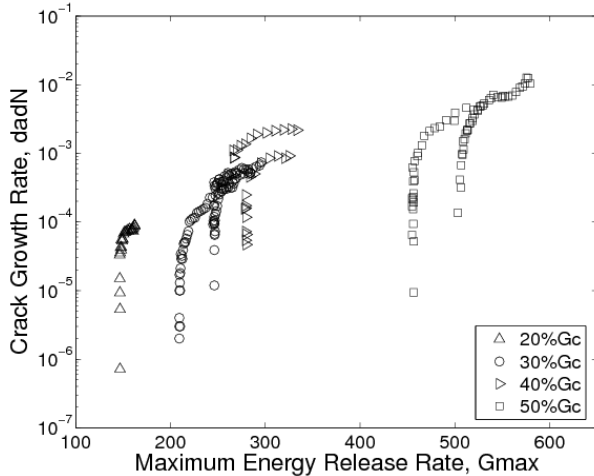


Figure 12. Crack growth rate for AS4/3501.

The mode II test is an unstable test. Once the crack starts growth reaches high energy release rate values quickly. The 3NF test has the limitation that when the crack length grow enough and arrives near the load applicator, local effects provide wrong experimental values. There is only a small range that can be used.

A threshold for each specimen corresponding the time before the crack starts to grow is observed. The Paris law could be determined but it would have to be done by parts, using some samples.

5. CONCLUSIONS

In conclusion, the new method presented permits the real time monitoring of the evolution of the compliance during a fatigue test. From the Compliance data stored continuously during the test, the $C(N)$ graph can be produced. With this graph, the onset point can be determined with the accuracy of one cycle. Then, the $a(N)$ graph results from fitting the $C(N)$ curve to a first order polynomial and the da/dN , is calculated. More experimental values of the da/dN - G_{max} graph are obtained with this method.

This new methodology reduces man-labour dependence and permits an automation of fatigue tests.

ACKNOWLEDGEMENTS

The authors would like to acknowledge in particular the Instituto Nacional de Técnica Aeroespacial, INTA for providing the samples. The authors also acknowledge

the Spanish Government for funding this work in the MAT2009-07918 project.

REFERENCES

- [1] ASTM D6115 - 97 *Standard Test Method for Mode I Fatigue Delamination Growth Onset of Unidirectional Fiber-Reinforced Polymer Matrix Composites* (2004).
- [2] S. Benmedakhene, M. Kenane, M.L. Benzeggagh (1999). *Initiation and growth of delamination in glass/epoxy composites subject to static and dynamic loading by acoustic emission monitoring*. Composite Science and Technology, 59:201-208.
- [3] H.Y. Ling, K.T. Lau, Z. Su, E.T.T. Wong (2007). *Monitoring mode II fracture behaviour of composite laminates using embedded fiber-optic sensors*. Composites: Part B, 38:488-497.
- [4] R. Schueler, S.P. Joshi, K. Schulte (2001). *Damage detection in CFRP by electrical conductivity mapping*. Composites Science and Technology, 61:921-930.
- [5] European Structural Integrity Society Polymers & Composites Task Group (1992). *Protocol for interlaminar fracture testing n° 2. Protocols for Interlaminar testing of Composites*.